2020 IEEE International Conference on Robotics and Automation (ICRA)
31 May - 31 August, 2020. Paris, France

A Novel Portable Lower Limb Exoskeleton for Gravity Compensation during Walking

Libo Zhou, Weihai Chen*, Wenjie Chen*, Shaoping Bai, and Jianhua Wang

Abstract—**This paper presents a novel portable passive lower limb exoskeleton for walking assistance. The exoskeleton is designed with built-in spring mechanisms at the hip and knee joints to realize gravity balancing of the human leg. A pair of mating gears is used to convert the tension force from the built-in springs into balancing torques at hip and knee joints for overcoming the influence of gravity. Such a design makes the exoskeleton has a compact layout with small protrusion, which improves its safety and user acceptance. In this paper, the design principle of gravity balancing is described. Simulation results show a significant reduction of driving torques at the limb joints. A prototype of single leg exoskeleton has been constructed and preliminary test results show the effectiveness of the exoskeleton.**

I. Introduction

Various lower limb exoskeletons have been developed for rehabilitation of patients with dyskinesia of lower limbs [1]-[4]. Exoskeletons can be grouped into powered exoskeletons and passive exoskeletons based on the usage of power method [4]. Powered exoskeletons are usually driven through electric motors or hydraulic cylinders with battery or external power as energy. Rehabilitation training by powered exoskeletons is intuitive and effective, and many powered exoskeletons have been developed [5]-[9]. A limitation of these exoskeletons is that they move in a predetermined trajectory rather than allowing the patients move under their own control. This prevents the patients to practice appropriate movement patterns according to their recovery situations to promote relearning of typical patterns. Passive exoskeletons do not require any external energy source, its movement is entirely dependent on the wearers own actions. Compared with powered exoskeletons, passive exoskeletons are usually lighter, cheaper and safer.

Passive exoskeletons are commonly designed with springs and the springs are used for two purposes. One is to store and return energy during each step. A representative passive exoskeleton was developed to aid ankle propulsion [10], [11]. The exoskeleton acts in parallel with the user's calf muscles and uses a passive mechanical clutch which consists of a ratchet and a pawl to engage the spring when the foot is on the ground and disengage it when the foot is in the air. Research results show that it helps to reduce the metabolic cost of walking by 7.2±2.6% for healthy people. A passive exoskeleton with elastic artificial tendons was proposed to minimize human joint work during walking in which artificial tendons act in parallel with the leg and are able to store and redistribute energy over the human lower limb joints [12]-[14].

The other purpose of the spring used in passive exoskeletons is to compensate the gravity of human body or human limbs. Research results show that passive exoskeletons with gravity compensation can significantly decrease users' muscular-actuation efforts and improve motor learning capability [15], [16]. A passive lower limb exoskeleton design composed of links and springs can be found in [16], [17]. In the design, a parallelogram mechanism was used to locate the centers of mass of the leg and the exoskeleton. The springs were then placed at suitable positions to compensate the gravity of the system. Another passive assistive device was proposed in [18] for sit-to-stand tasks. This device uses auxiliary parallelograms to obtain the center of mass of the human body which is modeled as having three degrees of freedom, and the springs are then added to make the total potential energy of the system constant during standing up. To overcome the gravity of human lower limb, multiple designs with elastic articulated cable have been proposed [19], including perfect gravity balancing of the limb using parallelogram with zero free length springs or four-bar mechanism with torsion springs, and the approximate gravity balancing of the limb with two different stiffness linear springs.

The working principle of passive exoskeletons is commonly based on the gravity balancing mechanism [20], [21], using spring to compensate the gravity of the load. This type of design has the advantage of being light. However, the design requires auxiliary instrumentation for real implementation, and the spring will occupy additional space around the balancer during the joint rotation. To avoid the potential interference between the mechanical parts, the spring is installed outside the linkages at a distance from the joint. Such design significantly increases the structure complexity of the exoskeleton and the outside spring increases the risk of possible harm to the wearer.

Some designs have tried to embed all mechanical elements inside the frames of the linkages. A new type interior cam mechanism which installed inside the main rotation joint was proposed as a gravity-balancing mechanism for robot arms [22]. A limitation of the design is that the cam contact may be unstable in dynamic situation. A new gravity compensation mechanism which consists of an embedded pulley system was developed for lower limb rehabilitation [23]. The spring is driven by the pulleys and is installed inside the frames of the linkages for a safe interaction with the wearer. A shortage of the balancer is that the design is complicated to include a bundle of pulleys and wires. A one-DoF gravity balancer designed with an inverted Cardan Gear Mechanism and a planetary gear train has been proposed in [24]. The design makes its mechanical components be integrated as a compound

This research is supported by supported by the National Natural Science Foundation of China under Grant No. 51975002 and 61773042.

Libo Zhou, Weihai Chen and Jianhua Wang are with the School of Automation Science and Electrical Engineering, Beihang University, BJ 100191, China (e-mail: libozhou@buaa.edu.cn; whchen@buaa.edu.cn; jhwangbuaa@126.com).

Wenjie Chen is with the School of Electrical Engineering and Automation, Anhui University, HF 230601, China (wjchen_ahu@126.com).

Shaoping Bai is with Department of Materials and Production, Aalborg University, Aalborg 9220, Denmark (e-mail: shb@mp.aau.dk).

*Corresponding author

rotating joint and achieve perfect static balancing using practical tensile spring. However, the free length of the spring should be equal to the radius of the ring gear in the Cardan gear mechanism, as the compensation of a larger gravity requires a stiffer spring with longer length, there is a compromise between the mechanism size and the compensation gravity. Besides, the proposed balancer is not suitable for lower limb exoskeleton due to the lack of adjustment mechanism for different weight subjects.

This paper presents a novel passive lower limb exoskeleton for walking assistance of people who lack of motor ability. The leg exoskeleton has two DoFs, one at the hip joint and the other at the knee joint. In the design, a pair of mating gears is used to convert the tension force generated by the springs into torques. All springs are mounted inside the frames of linkages in the thigh and the shank, which makes the exoskeleton has a compact layout with small protrusion. The pretension force of the springs can be adjusted by a lead screw nut mechanism to compensate the gravity for different subjects.

In this paper, the design principle is described in detail in Section II, which includes a design concept for perfect gravity balancing, followed by a simplified design with the parameters optimized for approximate gravity balancing. In Section III, simulations are conducted to show the performance of the simplified exoskeleton on the reduction of driving torque. A prototype of the simplified exoskeleton and preliminary test results are shown in Section IV followed by conclusions of this paper in Section V.

II. Working Principle of the New Design

A. Preliminary design for perfect gravity balancing

Our proposed exoskeleton is designed with linear springs for gravity compensation. The perfect gravity balancing is defined based on the condition that the overall potential energy of the human-exoskeleton system dependent on gravity and the springs remains constant during walking [21]. The basic components of the exoskeleton with a human leg are shown in Fig. 1 (a).

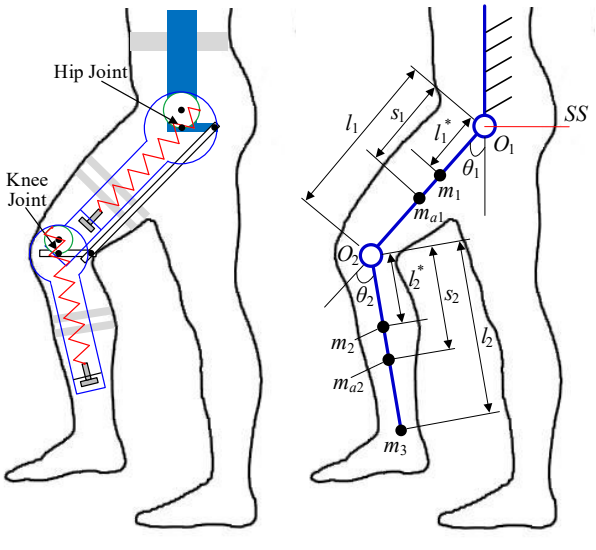

(a) (b)

Fig. 1. Model of the human-exoskeleton leg. (a) Basic components of the exoskeleton with a leg. (b) Various terms and parameters.

The leg is simplified as a two-linkage mechanism which stands for the thigh and the shank in the sagittal plane, and the foot is approximated as a point mass m_3. The model is shown in Fig. 1 (b), where *SS* is defined as the zero potential energy surface. The gravitational potential energy of the overall human-exoskeleton leg is

$$V_G = V_{Gt} + V_{Gs} + V_{Gf} \tag{1}$$

where V_{Gt}, V_{Gs}, and V_{Gf} are the gravitational potential energy of the thigh, shank and foot respectively, and can be obtained as

$$\begin{aligned} V_{Gt} &= -m_1 g l_1^* \cos\theta_1 - m_{a1} g s_1 \cos\theta_1 \\ V_{Gs} &= -m_2 g[l_2^* \cos(\theta_2 - \theta_1) + l_1 \cos\theta_1] \\ &\quad -m_{a2} g[s_2 \cos(\theta_2 - \theta_1) + l_1 \cos\theta_1] \\ V_{Gf} &= -m_3 g[l_2 \cos(\theta_2 - \theta_1) + l_1 \cos\theta_1] \end{aligned} \tag{2}$$

where m_1, m_2 and m_3 are the mass of the thigh, shank and foot of human leg respectively. m_{a1} and m_{a2} are the mass of the thigh and the shank of the exoskeleton respectively. l_1 and l_2 are the lengths of the thigh and the shank respectively. l_1^* and l_2^* are the distances of the center of mass (COM) of the thigh to the hip joint and the COM of the shank to the knee joint for the human leg respectively. s_1 and s_2 are the distances of the COM of the thigh to the hip joint and the COM of shank to the knee joint for the exoskeleton leg respectively. θ_1 and θ_2 are the rotation angles of the hip and knee joints respectively.

Equations (1) and (2) yield

$$V_G = H_1 \cos\theta_1 + H_2 \cos(\theta_2 - \theta_1) \tag{3}$$

with

$$\begin{aligned} H_1 &= -m_1 g l_1^* - m_{a1} g s_1 - (m_2 + m_{a2} + m_3) g l_1 \\ H_2 &= -m_2 g l_2^* - m_{a2} g l s_2 - m_3 g l_2 \end{aligned}$$

The working principle of a single joint is shown in Fig. 2. The design includes a pair of gear, a tension spring, two identical compression springs and an adjusting mechanism. Of the two gears, the pinion (the small gear) has a half of the diameter of the gear (the large gear). In the initial position shown in Fig. 2 (a), the tension spring is installed passing through the rotation centers of the two gears with one end attached at point *B* which is fixed in the adjustment mechanism and the other end attached at point *A* which is fixed on the pinion. The two identical compression springs are free with one end of the spring attached at point *C* or *D* which is fixed on the gear. The other end clinging to the driving point *E* which is fixed on the pinion. The adjusting mechanism is used to change the preload of the tension spring. According to the gear transmission relationship, the pinion rotates with the gear, and the points *A* and *E* trace a perfectly straight line [24], with the springs extended or compressed. All the three springs are designed with the same stiffness *k*, and an arbitrary operation state is shown in Fig. 2 (b).

When the gear rotates an angle θ_1, as shown in Fig. 2 (b), points *A* and *E* move distances Δl_1 and s_1 respectively, and the distances can be obtained as

$$\Delta l_1 = 2r(1 - \cos\theta_1) \tag{4}$$

$$s_1 = 2r\sin\theta_1 \tag{5}$$

where *r* is the radius of the pinion.

For the tension spring, its elastic potential energy when the gear at angle θ_1 is

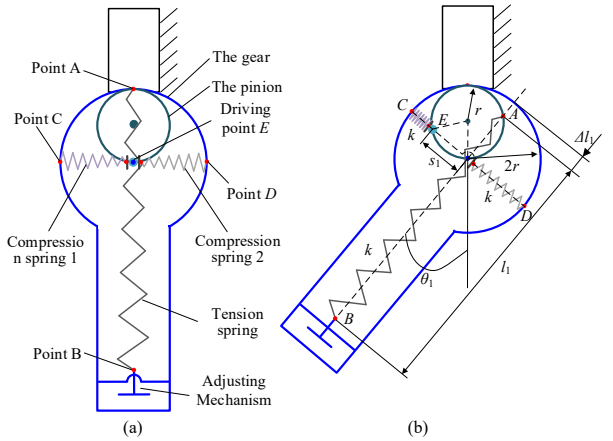

Fig. 2. Basic working principle of the design. (a) Initial position. (b) Rotates at an arbitrary angle θ_1.

$$E_t = \frac{k}{2}(C_0 - \Delta l_1)^2 \tag{6}$$

where C_0 is the deformation of the spring due to the pretension force at initial position.

For the compression spring, it is free at the initial position, and its elastic potential energy at angle θ_1 is

$$E_c = \frac{k}{2}{s_1}^2 \tag{7}$$

The overall elastic potential energy due to the springs is

$$E = E_t + E_c \tag{8}$$

Combining Eq. (4)-Eq. (8), the elastic potential energy E is

$$E = 2kr(C_0 - 2r)\cos\theta_1 + 2kr^2 + \frac{k}{2}(C_0 - 2r)^2 \tag{9}$$

A kinematic representation of the lower limb exoskeleton robot is shown in Fig. 3 (a). It includes a 1-DOF hip joint module and a 1-DOF knee joint module. As the motion of the knee joint is in single direction which referred as flexion motion while the motion of the hip joint includes both flexion and extension motions, only one compression spring is installed in the knee joint and two identical compression springs are installed in the hip joint. A lightweight auxiliary link is designed in parallel with the thigh, and thus a parallelogram mechanism with its rotation joints at point $O, H_1, H_2,$ and H_3 is formed. The parallelogram mechanism can ensure the knee base is parallel to the hip base which is in a horizontal position.

Referring to the kinematic model shown in Fig. 3 (a), where $x - O - y$ is the fixed-coordinate frame with its original located at point *O*. The horizontal plane which goes through the x-axis is defined as the zero potential energy surface. Thus, the rotation angles of the gears in the hip and knee joints are θ_1 and $\theta_3 = \theta_2 - \theta_1$.

Referring to Eq. (3) and Eq. (9), we can get the total potential energy of the human-exoskeleton system is

$$P = (H_1 + J_1)\cos\theta_1 + (H_2 + J_2)\cos(\theta_2 - \theta_1) + P_0 \tag{10}$$

with

$$H_1 = -m_1 g l_1^* - m_{a1} g s_1 - (m_2 + m_{a2} + m_3) g l_1$$
$$H_2 = -m_2 g l_2^* - m_{a2} g s_2 - m_3 g l_1$$
$$J_1 = 2k_1 r_1 (C_{01} - 2r_1)$$
$$J_2 = 2k_2 r_2 (C_{02} - 2r_2)$$

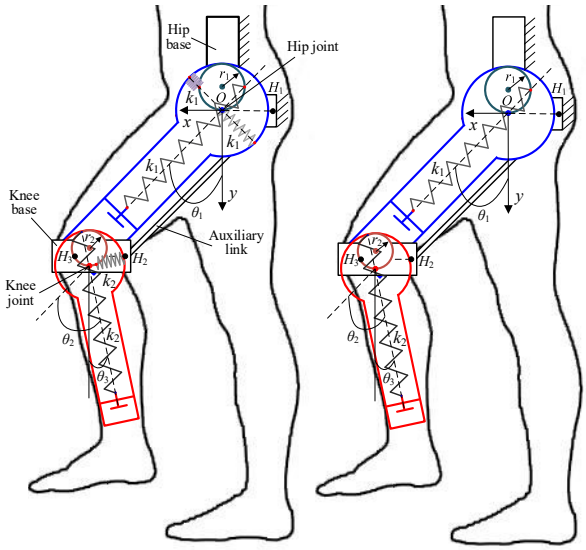

Fig. 3. Kinematic model of the lower limb exoskeleton. (a) Original design for gravity compensation. (b) Simplified design for approximate gravity compensation.

$$P_0 = 2k_1 {r_1}^2 + \frac{k_1}{2}(C_{01} - 2r_1)^2 + 2k_2 {r_2}^2 + \frac{k_2}{2}(C_{02} - 2r_2)^2$$

where k_1 and k_2 are the stiffness of the springs, r_1 and r_2 are the radii of the pinions in the hip and knee joints respectively. C_{01} and C_{02} are the initial deformations of the tension springs in the thigh and the shank respectively. The other parameters of H_1 and H_2 are defined in Eq. (2).

From Eq. (10), we can find that if the coefficients of terms containing trigonometric variables vanish, i.e., $H_1 + J_1 = H_2 + J_2 = 0$, then the total potential energy is given by $P = P_0$, which is a constant. Therefore, the total potential energy becomes configuration independent, and a perfect gravity balancing is achieved. These conditions yield

$$k_1 = \frac{m_1 g l_1^* + m_{a1} g s_1 + (m_2 + m_{a2} + m_3) g l_1}{2r_1(C_{01} - 2r_1)}$$
$$k_2 = \frac{m_2 g l_2^* + m_{a2} g l s_2 + m_3 g l_2}{2r_2(C_{02} - 2r_2)} \tag{11}$$

Hence, if the springs with stiffness given by (11) are used, the mechanism can realize gravity-balanced. After the springs are selected, the initial deformations of the tension springs C_{01} and C_{02} can be adjusted to vary the level of gravity balancing.

B. Approximate Gravity Balancing for Lower Limb

The method presented above provides a perfect gravity balancing system with built-in springs for the leg. A limitation of the method is that it requires both tension springs and compression springs and these must have the same stiffness for each joint. This section presents a method for approximate gravity balancing of leg with only tension springs, which makes the proposed design more compact than the previous ones. The parameters of the design are optimized to minimize the variations of the total potential energy of the human-exoskeleton leg.

Fig. 3 (b) shows the model of the simplified lower limb exoskeleton. Compared with the previous design shown in Fig. 3 (a), only a tension spring is used for each joint in this

design. Through Eq. (4) and Eq. (6), the overall elastic potential energy of the exoskeleton is

$$E = A_1\cos\theta_1 + A_2\cos^2\theta_1 + B_1(\theta_2 - \theta_1) + B_2\cos^2(\theta_2 - \theta_1) + E_{01} + E_{02} \quad (12)$$

with

$$A_1 = 2k_1r_1(C_{01} - 2r_1)$$
$$A_2 = 2k_1{r_1}^2$$
$$B_1 = 2k_2r_2(C_{02} - 2r_2)$$
$$B_2 = 2k_2{r_2}^2$$
$$E_{01} = \frac{k_1}{2}(C_{01} - 2r_1)^2$$
$$E_{02} = \frac{k_2}{2}(C_{02} - 2r_2)^2$$

The total potential energy of the human-exoskeleton is

$$Q = (A_1 + H_1)\cos\theta_1 + A_2\cos^2\theta_1 + E_{01} + (B_1 + H_2)\cos(\theta_2 - \theta_1) + B_2\cos^2(\theta_2 - \theta_1) + E_{02} \quad (13)$$

where parameters of A_1, A_2, B_1, B_2, H_1, H_2, E_{01} and E_{02} are defined in Eq. (3) and Eq. (13).

Variation of the total potential energy of the human-exoskeleton system leads to the increment of the balancing torque at human lower limb joints. To reduce this torque increment, the variation of the total potential energy Q should be minimized for the whole walking gait.

As shown in Eq. (13), the total potential energy Q is a function of the hip and knee joints angle variables $\{\theta_1, \theta_2\}$, and also of the design parameters such as the radii of the pinions r_1 and r_2, the initial deformations of the tension springs C_{01} and C_{02}, and the spring stiffness k_1 and k_2. It is necessary to find the suitable design parameters to minimize the variation of the total potential energy.

Hence, the total potential energy at n points among the whole walking gait cycle $\{\theta_1, \theta_2\}$ is evaluated, named Q_k, and the average potential energy of the n points are then calculated, defined as $\bar{Q}$. The optimization problem is

$$min\ \frac{\sum_{k=1}^{n}(Q_k - \bar{Q})^2}{n-1}$$
$$S.T.\ k_i > 0, C_{0i} > 0, r_i > 0, i = 1,2. \quad (14)$$

III. Simulations with MATLAB/SimMechanics

A CAD model of the simplified lower limb exoskeleton was built by Solidworks, as shown in Fig. 4. The spring is connected with the pinion by a wire rope. The adjusting mechanism is a lead screw nut mechanism which can be used to adjust the initial deformation of the tension spring. A length adjusting mechanism with double guide rods was designed for the adjustment of the thigh length and two ultra-small magnetic encoder sensors are installed to measure the rotation angles of the hip and knee joints. The design parameters of the exoskeleton are listed in Table I.

The exoskeleton was then attached to a human model. The parameters of the mass and the center-of-mass of the human-exoskeleton model obtained in the Solidworks are shown in Table II. The human-exoskeleton model was then imported into SimMechanics for simulation. In the simulation, the input signals are the trajectories of hip and knee joints according to the general human gait [2], [25] and the initial deformations of the tension springs in the thigh and the shank are obtained after optimization shown in Eq. (14). The torque additional required at the human joints to drive the limbs was obtained to show the performance of the exoskeleton.

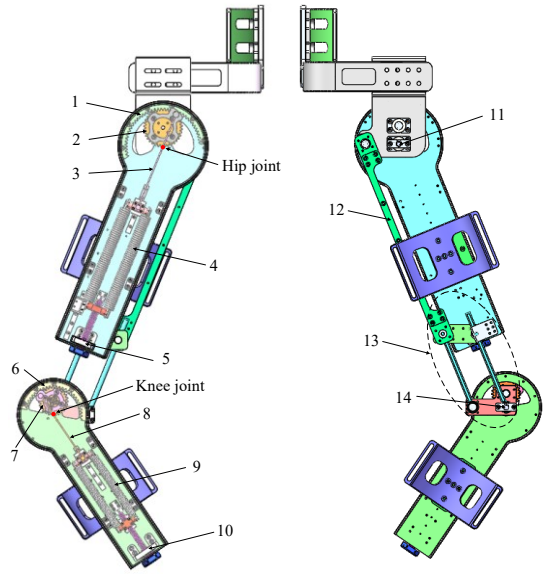

Fig. 4. Mechanism model of the exoskeleton. (a) Front view. (b) Rear view. 1-Gear 1, 2-Pinion 1, 3-Wirerope 1, 4-Tension spring 1, 5-Adjusting mechanism 1, 6-Gear 2, 7-Pinion 2, 8-Wirerope 2, 9-Tension spring 2, 10-Adjusting mechanism 2, 11-Encoder sensor 1, 12-Auxiliary link, 13-Length adjusting mechanism, 14-Encoder sensor 2.

The variations of torques at the limb joints during a gait cycle are shown in Fig. 5. It can be seen that for the unbalanced human-exoskeleton system of which the spring stiffness is set as zero, the maximum torque to drive the lower limb is about 15 Nm for the hip joint and 6 Nm for the knee joint. It also reaches nearly 15 Nm and 5.5 Nm for the hip joint and knee joint respectively without exoskeleton. For the balanced human- exoskeleton system, we can find that the maximum torque is reduced to about 3.5 Nm for the hip joint and 1.5 Nm for the knee joint, which is only about one quarter of the maximum torque when the human-exoskeleton system is unbalanced. The averaged absolute values of the torque at the hip and knee joints are shown in Fig. 6. We can find that the average absolute torques are reduced from 6.95 Nm (without exoskeleton) to 1.46 Nm for the hip joint and 2.22 Nm (without exoskeleton) to 0.74 Nm for the knee joint.

TABLE I. Parameters of the Developed Lower Limb Exoskeleton

Param.	Value	Param.	Value
Radius of pinion 1 (mm)	27	Radius of pinion 2 (mm)	20.25
Original length of tension spring 1 (mm)	150	Original length of tension spring 2 (mm)	100
Stiffness of tension spring 1 (N/mm)	10.79	Stiffness of tension spring 2 (N/mm)	6.75
Initial tension of tension spring 1 (N)	123.6	Initial tension of tension spring 2 (N)	34.3

TABLE II. Parameters of the Human-Exoskeleton System in the Simulations

Param.	Value	Param.	Value	Param.	Value
m_1	6.838 kg	m_2	3.102 kg	m_3	0.846 kg
m_{a1}	1.060 kg	m_{a2}	0.628 kg	l_1	440 mm
l_2	400 mm	l_1^*	194 mm	l_2^*	179 mm
s_1	173 mm	s_2	104 mm	g	9.8 N/kg

All parameters are defined in Section II. A.

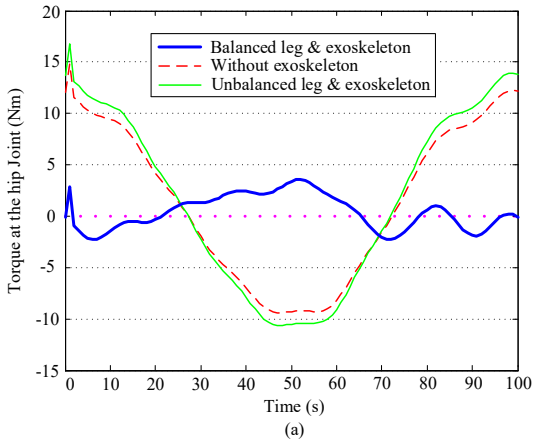

(a)

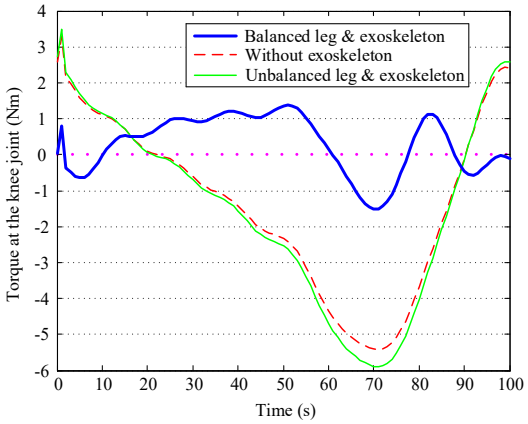

(b)

Fig. 5. Varying torques required at the lower limb joints. (a) At the hip joint. (b) At the knee joint. The period length of the gait cycle is 5 s.

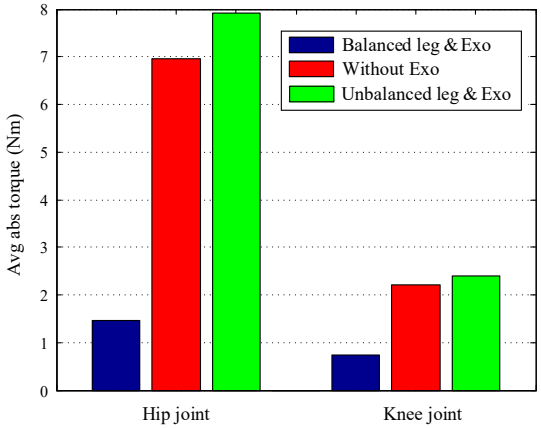

Fig. 6. Average absolute torque at the human hip and knee joints.

IV. Prototyping and Experiment

A. Characterization Experiment

The designs of the hip joint and knee joint share the same working principle. A characterization experiment on a single joint was conducted to verify the performance of the design. The parameters of the designed joint are shown in Table III and the experiment setup is shown in Fig. 7. An index plate with mounting holes at intervals of 10 degrees was installed and fixed in the base. The fixing connecting bar can be fixed at different positions through the mounting holes. A Force/Torque sensor (ATI MINI 45) was installed to measure the assistive force provided by the designed mechanism with a maximum force of 145 N and a resolution of 1/128 N. The data of the measured force was then transformed to the torque at the joint multiplied by the arm of the force. The experiments were conducted when the initial deformation of the spring is set as 0 mm, 10 mm, 20 mm, and 40 mm and the data was recorded at intervals of 10 degrees when the springs are under tension. It is noted that when the initial deformation of the spring is 0 mm, the data measured reflects the torque that overcomes the gravity of the prototype.

Fig. 8 shows the torque provided by the designed mechanism. It should be noted that the data when the spring is free is not recorded during the experiment. As seen in Fig. 8, the experimental results are generally in accordance with the desired torque. The errors are small, which are mainly due to the physical limitations of the test platform, such as gear backlash, internal friction and material deformation.

TABLE III. Parameters of The Developed One DoF Prototype.

Param.	Value	Param.	Value
Radius of pinion (mm)	20.25	Original length of tension spring (mm)	100
Stiffness of tension spring (N/mm)	0.56	Initial tension of tension spring (N)	10.49

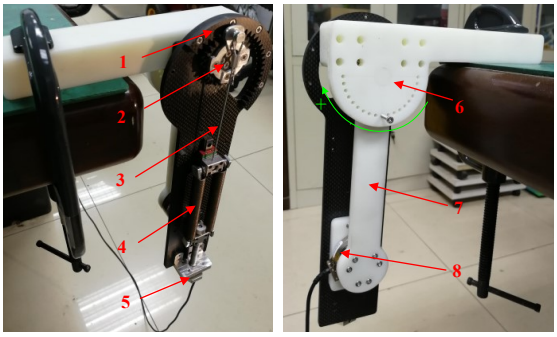

(a) (b)

Fig. 7. Test platform for a single joint. (a) Front view. (b) Rear view. The green arrow in (b) indicates the positive direction. 1- Pinion, 2- Gear, 3-Wirerope, 4-Tension spring, 5-Preload adjusting mechanism, 6-Index plate, 7- Fixing connecting bar, 8-Force/Torque sensor.

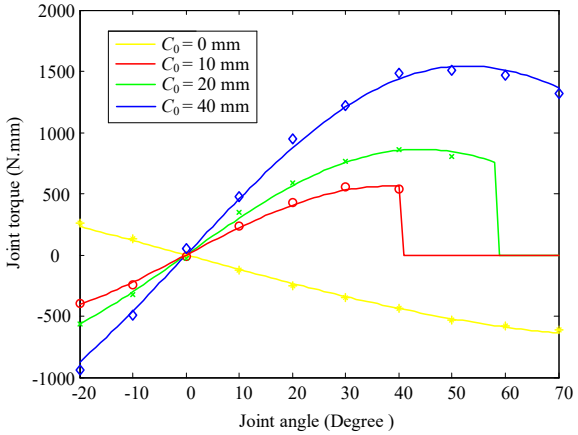

Fig. 8. Experimental results of the torque versus the angle of the joint. The solid lines stand for the desired torque while the scattered points stand for the measured torque at several positions when C_0 =10 mm, 20 mm, and 40mm. The solid line for C_0 = 0 is T = -680 sinθ_1, which is the fitting curve of the measured data. The desired torque is obtained by differential of Eq. (6).

(a) (b) (c) (d)

Fig. 9. Photographs of the exoskeleton prototype with a subject. (a) Standing position. (b) Leg flexion position. (c) Leg extension position. (d) With a shell mounted.

B. Prototype

A prototype with only one leg has been developed with the dimensions of the prototype are described in Table I. The prototype is made of resin, carbon fiber plate and aluminum and its weight is about 2.2kg. This leg exoskeleton fits persons from 1.60 m to 1.90 m tall, which covers more than 90% of corresponding adult males [26]. Usability testing on Standing position, Leg flexion position, Leg extension position has been conducted on a healthy subject (Male, 25 years old, 180 cm in height, 63 kg in weight), as shown in Fig. 9.

V. Conclusion

This paper presents a novel design of a portable passive lower limb exoskeleton for gravity balancing of a human leg during walking. The design features the capability of balancing the gravity of lower limb with built-in spring mechanisms. In this work, the design principle of gravity balancing is described. A model of the human-exoskeleton system is developed and validated by numerical simulations. A characterization experiment on a single joint is conducted to verify the performance of the design followed by a prototype of single leg exoskeleton with usability tests to show its effectiveness.

The main contribution of the work lies in the novel design of an exoskeleton with built-in spring mechanisms for gravity balancing. This enables the springs embedded inside the frames of linkages in the thigh and the shank, which makes the exoskeleton has a compact layout with small protrusion. Future research work will focus on the quantitative evaluations of the exoskeleton, such as the acquisition of electromyography data involved in the movement of leg. Besides, the exoskeleton is to be constructed with two legs, and the metabolic cost of human will be measured to verify its performance.

References

[1] S. Bai, G. S. Virk and T. Sugar, *Wearable Exoskeleton Systems: Design, Control and Applications*, Institution of Engineering & Technology, 2018, pp. 5-50.

[2] L. Zhou, W. Chen, J. Wang, S. Bai, H. Yu, and Y. Zhang, "A Novel Precision Measuring Parallel Mechanism for the Closed-loop Control of a Biologically Inspired Lower Limb Exoskeleton, " *IEEE/ASME Trans. Mechatron.*, vol. 23, no. 6, pp. 2693-2703, Dec. 2018.

[3] W. Meng, Q. Liu, Z. Zhou, Q. Ai, B. Sheng, and S. Xie, "Recent development of mechanisms and strategies for robot-assisted lower limb rehabilitation," *Mechatronics*, vol. 31, pp. 132–145, 2015.

[4] Z. Lovrenovic, and M. Doumit, "Review and analysis of recent development of lower extremity exoskeletons for walking assist," *IEEE EMBS Int. Student Conf. (ISC)*, Ottawa, Canada, May 29-31, 2016, pp.1-4.

[5] M. Talaty, A. Esquenazi, and J. E. Briceño, "Differentiating ability in users of the RewalkTM Powered Exoskeleton: An analysis of walking kinematics," *in Proc. IEEE Int. Conf. Rehabil. Robot.*, Seattle, WA, Jun. 24-26, 2013, pp.1-5.

[6] A. Tsukahara, Y. Hasegawa, K. Eguchi, Y. Sankai, "Restoration of gait for spinal cord injury patients using HAL with intention estimator for preferable swing speed," *IEEE Trans. Neural Syst. Rehabil. Eng.*, vol. 23, no. 2, pp. 308-318, Mar. 2015.

[7] Y. T. Pan, Z. Lamb, J. Macievich, and K. A. Strausser, "A vibrotactile feedback device for balance rehabilitation in the EksoGTTM robotic exoskeleton," *in Proc. IEEE Int. Conf. Biomed. Robot. Biomechatronics*, Enschede, The Netherlands, Aug. 26-29, 2018, pp.569-576.

[8] M. Munera, A. Marroquin, L. Jimenez, J. S. Lara, C. Gomez, S. Rodriguez, L. E. Rodriguze, and C. A. Cifuentes, "Lokomat therapy in Colombia: current state and cognitive aspects," *in Proc. IEEE Int. Conf. Rehabil. Robot.*, London, UK, July 17 -20, 2017, pp. 394-399.

[9] Y. Stauffer, Y. Allemand, M. Bouri, J. Fournier, R. Clavel, P. Metrailler, R. Brodard, and F. Reynard, "The WalkTrainer—A New Generation of Walking Reeducation Device Combining Orthoses and Muscle Stimulation," *IEEE Trans. Neural Syst. Rehabil. Eng.*, vol. 17, no. 1, pp. 38-45, Feb. 2009.

[10] M. B. Wiggin, G. S. Sawicki, S. H. Collins, "An exoskeleton using controlled energy storage and release to aid ankle propulsion," *in Proc. IEEE Int. Conf. Rehabil. Robot.*, ETH Zurich Science City, Switzerland, Jun. 29-Jul. 1, 2011, pp.1-5.

[11] S. H. Collins, M. B. Wiggin, and G. S. Sawicki, "Reducing the energy cost of human walking using an unpowered exoskeleton," *Nature*, vol. 522, no. 7555, pp. 212–215, Jun. 2015.

[12] A. J. van den Bogert, "Exotendons for assistance of human locomotion," *Biomed. Eng. Online,* vol. 2, p. 17, Oct. 2003.

[13] W. van Dijk, H. van der Kooij, and E. Hekman, "A passive exoskeleton with artificial tendons: Design and experimental evaluation," *in Proc. IEEE Int. Conf. Rehabil. Robot.*, ETH Zurich, Switzerland, Jun. 27- Jul. 01, 2011, pp. 1–6.

[14] W. van Dijk and H. V. der Kooij, "XPED2: A passive exoskeleton with artificial tendons," *IEEE Robot. Autom. Mag.*, vol. 21, no. 4, pp. 56–61, Dec. 2014.

[15] T. Rahman, W. Sample, R. Seliktar, M. T. Scavina, A. L. Clark, K. Moran, and M. A. Alexander, "Design and Testing of a Functional Arm Orthosis in Patients With Neuromuscular Diseases," *IEEE Trans. Neural Syst. Rehabil. Eng.,* vol. 15, no. 2, pp. 244-251, Jun. 2007.

[16] S. K. Banala, S. K. Agrawal, A. Fattah, V. Krishnamoorthy, W. L. Hsu, J. Scholz, and K. Rudolph, "Gravity-Balancing Leg Orthosis and Its Performance Evaluation," *IEEE Trans. Robot.,* vol. 22, no.6, pp.1228-1239, Dec. 2006.

[17] S. K. Agrawal, and A. Fattah, "Theory and design of an orthotic device for full or partial gravity-balancing of a human leg during motion," *IEEE Trans. Neural Syst. Rehabil. Eng.,* vol. 12, no. 2, pp. 157-165, Jun. 2004.

[18] A. Fattah, S. K. Agrawal, G. Catlin, and J. Hamnett, "Design of a passive gravity-balanced assistive device for sit-to-stand tasks," *J. Mech. Des.*, vol. 128, no.5, pp. 1122-1129, Sep. 2006.

[19] A. Alamdari, R. Haghighi, and V. Krovi, "Gravity-balancing of elastic articulated-cable leg-orthosis emulator," *Mech. Mach. Theory*, vol. 131, pp.351-370, Jan. 2019.

[20] R. H. Nathan, "A constant force generation mechanism," *ASME J. Mech. Transm. Autom. Des.*, vol. 107, no.4, pp. 508-512, Dec. 1985.

[21] V. Arakelian, "Gravity compensation in robotics," *Adv. Robot.* vol. 30, no. 2, pp. 79-96.

[22] K. Koser, "A cam mechanism for gravity-balancing," *Mech. Res. Commun.*, vol. 36, no. 4, pp. 523-530, Jun. 2009.

[23] T. Nakayama, Y. Araki, and H. Fujimoto, "A new gravity compensation mechanism for lower limb rehabilitation," *in Proc. IEEE Int. Conf. Mechatron.Autom.*, Changchun, China, Aug. 9- 12, 2009, pp. 943-948.

[24] Y. C. Hung and C. H. Kuo, "A novel one-DoF gravity balancer based on cardan gear mechanism," *in New Trends in Mechanism and Machine Science: Theory and Industrial Applications*, P. Wenger, and P. Flores, Eds, Springer International Publishing Switzerland 2017 pp. 261-268.

[25] J. Perry MD, *Gait Analysis: Normal and Pathological Function*, Slack Incorporated, Thorofare, 1992, pp. 309–311.

[26] R. L. Huston, *Principles of Biomechanics*, CRC Press, Boca Raton, 2009, pp. 24-26.